

Document downloaded from:

<http://hdl.handle.net/10251/101670>

This paper must be cited as:



The final publication is available at

<http://doi.org/10.1038/nature07957>

Copyright © Nature Publishing Group

Additional Information

ITQ-37 a chiral zeolite framework following the SrSi₂ net and containing 30-ring extra-large gyroidal channels

Junliang Sun¹, Charlotte Bonneau¹, Ángel Cantín², Avelino Corma², María J. Díaz-Cabañas², Manuel Moliner², Daliang Zhang¹, Mingrun Li¹ and Xiaodong Zou¹

¹Structural Chemistry and Berzelii Centre EXSELENT on Porous Materials, Stockholm University, SE-106 91 Stockholm, Sweden

²Instituto de Tecnología Química (UPV-CSIC), Av. Naranjos s/n, E-46022 Valencia, Spain

The synthesis of crystalline molecular sieves with pore dimensions that fill the gap between microporous and mesoporous materials is a matter of fundamental and industrial interest.¹⁻³ If zeolites with extra-large pores and chiral frameworks could be prepared, it will open new perspectives for zeolitic materials and their applications. Two important steps along the above direction include the synthesis of ITQ-33 with 18×10×10 ring windows stable zeolite,⁴ and the synthesis of SU-32⁵ in where each crystal exhibits only one handedness and has an intrinsically chiral zeolite structure. Here we present a silicogermanate zeolite (ITQ-37) with extra-large 30-ring windows, which structure was determined by combining selected area electron diffraction (SAED) and powder X-ray diffraction (PXRD) in a charge-flipping algorithm.⁶ The framework follows the SrSi₂ (srs) minimal net⁷ and forms two unique cavities where each cavity is connected to three other cavities to form a gyroidal channel system. These cavities describe the enantiomorphous srs net of the framework. ITQ-37 is the first chiral zeolite with one single gyroidal channel. It has the lowest framework density (10.3 T atoms per 1000Å³) of existing 4-coordinated crystalline oxide frameworks, and the pore volume of the corresponding silica polymorph would be 0.38 cc.g⁻¹.

Three-dimensional extra-large pore systems have been the realm of amorphous silica materials with wall structures corresponding to the primitive (P), diamondoid (D) and gyroidal (G) periodic surfaces, with a significant higher occurrence of the G-surface; only the latter exhibits chiral channels of opposite handedness on either side of the surface. The greater stability of the G-surface has been demonstrated mathematically⁸ and is understood in the chemistry of mesoporous silica materials, as a favourable configuration to lower the interface area between

hydrophobic and hydrophilic chemical domains during the formation of the crystal, thus minimising the energy at the interface. With inorganic crystalline compounds, the ANA⁹ framework remained the only zeolite following the G-surface until the discovery of UCSB-7¹⁰ with 12-ring channels. The first crystalline oxide synthesised with pores in the 20 Å range was SU-M,¹¹ which also exhibits a framework describing a reticulation of the G-surface. If the G-surface favours extra large pores, the specificity of structural chirality is only fulfilled in SU-MB, where Ge₇O₁₆F₃ clusters obstruct one of the gyroidal channels. Synthesising a compound with the inorganic framework on one side of the G-surface, whilst the other side remains vacant, constitutes a sensible route to achieve both three-dimensional channels displaying only one enantiomorph and extra large pores. ITQ-37 is the first zeolite corresponding to this configuration.

The germanosilicate ITQ-37 crystallizes in a cubic chiral space group (*P4₁32* or *P4₃32*, *a* = 26.5178(3) Å). All Si and Ge atoms are tetrahedrally coordinated with oxygen. The framework is built from single unique tertiary building units T₄₄O₁₄₅(OH)₇ (T = Si, Ge) that follows a three-coordinated **srs** net (Fig. 1).¹² There are eight such tertiary building units per unit cell, which lie on the nodes of the **srs** net (Fig. 1b). The framework generates a gyroidal channel system corresponding to the enantiomorph of its **srs** net (Fig. 1c). The gyroidal channel system consists of two unique large cavities at the 4*a* and 4*b* positions (with coordinates 3/8, 3/8, 3/8 and 7/8, 7/8, 7/8 and their symmetry equivalents). Each large cavity communicates with three others through windows of thirty TO₄ tetrahedra (30-rings) with an asymmetric opening of 4.7 x 19.7 Å (Fig. 1b and Supplementary Fig. S1), assuming the van der Waals diameter of oxygen 2.7 Å. Each tertiary building unit is itself composed from reoccurring motifs in zeolitic materials: one unique 4²6⁴ cage (lau) and two unique double 4-rings (Fig. 1b). One set of double 4-rings (D4R1) includes one terminal hydroxyl group while the second set (D4R2) exhibits two. The tertiary building unit is further linked to three neighbouring building units, by sharing a common D4R2 and half of a 6-ring of the lau cage. The D4R1s, D4R2s and the lau cages individually follow respectively the **srs**, **srs-e (lcv)** and **srs-a** nets.^{11,12} All of which are chiral and of the same handedness as the overall structure.

ITQ-37 is the first chiral zeolite with one single gyroidal channel. It has the lowest framework density of all existing 4-coordinated oxide frameworks, 10.3 T-atoms per 1000 Å³. The division of space in tiles represents a valuable tool to discern the structure. The tertiary building unit that forms the framework is constructed of five different tiles: two corresponding to

the D4Rs, one to the lau cage (**t-lau**) and two interfacial tiles (6^3 , **t-kah**) between the **t-lau** tiles (Fig. 2a and 2b). The channel system is constructed of three tiles: two large tiles with similar volumes corresponding to the large cavities (Fig. 2c) and an interfacial tile (for detailed tiling information see Supplementary Fig. S2). The tiling clearly demonstrates the opposite handedness of the channel system and the framework in ITQ-37 (Fig. 2c). It also offers a direct appreciation of the large accessible volume (Fig. 2d and Supplementary Movie S1). Determined from the N₂ isotherm (Figure S3), the BET surface area is 690 m²·g⁻¹, with 0.29 cc·g⁻¹ of micropore volume. Note that, these values would correspond to 900 m²·g⁻¹ BET and 0.38 cc·g⁻¹ for the silica polymorph of ITQ-37, which are far beyond any value previously reported for any zeolite structure.

Three large dicationic Organic Structure Directing Agent (OSDA) were synthesized by Diels-Alder reaction (see experimental in Supplementary Material and Supplementary Fig. S4). High throughput (HT) techniques in the synthesis of germanosilicates using the OSDAs allowed establishing phase diagrams showing that SDA1 and SDA3 gave Beta type materials or clathrasils, whereas SDA2 produced ITQ-24¹³ or a mixture of ITQ-24 with a new phase that we denoted as ITQ-37. Experimental conditions that lead to pure ITQ-37 were subsequently found. The details for the HT, the synthesis optimisation and the corresponding PXRD profiles are provided in the supplementary information (Supplementary Table S1, Table S2 and Fig. S5 and S6). The pure ITQ-37 was obtained with the following composition: [(C₂₂N₂H₄₀)_{10.5}(H₂O)_x][Ge₈₀Si₁₁₂O₄₀₀H₃₂F₂₀]. The number of SDA2 molecules (=10.5) in the structure was determined by elemental analysis. A single resonance in the ¹⁹F MAS-NMR spectrum at -10ppm is observed, which is assigned to fluoride anions entrapped in germanium rich D4R cages (Supplementary Fig. S7). The ²⁹Si MAS NMR spectra of the as-made ITQ-33 zeolite (Supplementary Fig. S8) shows two peaks at -94 and -96 ppm, which correspond to structural defects in different crystallographic position as confirmed by CP 1H MAS NMR spectrum.

The complexity of the ITQ-37 structure and the small crystal size (70-200 nm, Supplementary Fig. S9), plus the high-degree of overlapping reflections (> 94% exact overlapping with $d > 1.2$ Å) posed great challenges for the structure determination. Several complex zeolite structures were recently determined by combining transmission electron microscopy (TEM) and powder X-ray diffraction (PXRD).¹⁴⁻¹⁶ Crystal structure factor phases

obtained from high resolution electron microscopy (HRTEM) images were used to facilitate the structure solution from PXRD, by the FOCUS program¹⁷ based on crystal chemical information or the Superflip program based on charge-flipping algorithm.¹⁸ The presence of terminal hydroxyl groups on both silicon and germanium atoms made ITQ-37 significantly more electron beam sensitive than other zeolites. HRTEM images of ITQ-37 only allowed the observation of the approximate pore structure (Supplementary Fig. S10).

A new strategy combining SAED and PXRD was developed for solving the structure since SAED extends to a higher resolution than HRTEM images (Supplementary Fig. S10). Intensities of reflections were extracted from the SAED patterns along the [1 0 0], [1 1 0], [1 1 1] and [1 2 0] directions using the program ELD.¹⁹ These reflections cover about 80% of the total unique reflections to 3.3 Å resolution, and their intensities were used for the pre-repartitioning of overlapping reflections in PXRD. Among sixteen overlapping reflection groups below 26° of 2θ, ten of them were significantly changed by this pre-repartitioning, and became much closer to the structure factor intensities of the final structure. The charge flipping algorithm was then applied for structure determination combined with further repartitioning of overlapping reflections by histogram matching.²⁰ After a hundred runs of charge flipping iterations using the Superflip program,²⁰ the ten best results gave *R*-factors of about 25% and six of them showed similar electron density distribution as given in Fig. 3. In total, ten unique T atoms and eighteen unique oxygen atoms were automatically assigned by the EDMA program. One oxygen atom between T4 and T5 ($d_{T4-T5} = 3.6$ Å) was obviously missing and thus added manually. The resulting structure is a 3D tetrahedral framework, where all T-T and T-O distances are reasonable, except for the T4-T5 distance. The pore structure agrees with that observed in the HRTEM images (Supplementary Fig. S10). Note that we also tried the charge-flipping iterations without the pre-repartitioning and the correct model could also be obtained. However, the convergence was slower and decreased the chances of obtaining a proper model. The final framework structure was refined by Rietveld refinement with $R_p = 0.0314$, $R_{wp} = 0.0328$ and $\chi^2 = 5.04$ in Fig. 4 (see detailed crystallographic information in Table S3 and bond distances in Table S4).

In addition to extra-large pores, ITQ-37 shows a good thermal stability. A pelletized sample of ITQ-37 is stable after calcination at 813K (see Fig. S11) and remains stable for, at least, two weeks when stored at room temperature in moisture free environment. On the contrary, when exposed to 90% humidity at room temperature 20 and 50% of crystallinity is lost after 10 and 24

hours, respectively. Thus, catalytic tests were performed for Al-containing ITQ-37 ($T^{IV}/T^{III}=70$). The Al is tetrahedrally coordinated (see Fig. S12) and presents Brönsted acidity. The beneficial catalytic effect of the large pores has been shown by performing the acetalization of aldehydes of different molecular size with triethyl orthoformate. The catalytic results are compared in Table S5 with those obtained with zeolite Beta of a Si/Al ratio of 50. It can be seen that for the smaller aldehyde (heptanal) that can diffuse in the pores of Beta, both zeolites give similar initial activity (measured as mol converted per mol of Al and hour). However for larger aldehyde (diphenylacetaldehyde), the initial activity of ITQ-37 is almost three times that of Beta. Furthermore, the selectivity to acetal at high conversion is much better for ITQ-37 with the bulkier aldehyde.

With expert structure solution techniques, we have looked upon a chiral zeolite with a single extra large gyroidal channel intimately related to the G-minimal surface. With ITQ-37, we are reaching the domain of mesostructures of a zeolitic nature. This prompts to question the conventional models associated with both zeolite and mesoporous syntheses. The exploration of the chemistry involving larger non-surfactant molecules as OSDA could provide answers.

METHODS SUMMARY

Topological Analysis. The embedding of the tetrahedral net and tiling visualisation were performed by Systre²¹ and 3dt,²² respectively; both are part of the GAVROG project. The tiling data was computed with TOPOS.²³

TEM characterization. TEM work was performed on JEM3010 electron microscopes under low-dose conditions (Supplementary Fig. S10). The 4- and 6-fold symmetries in SAED patterns indicate a cubic cell. The unit cell was determined from SAED patterns and further refined by PXRD to be $a = 26.5178(3)$ Å. The reflection condition $h00: h=4n$ indicates that the space group is $P4_132$ or $P4_332$ (chiral with opposite handedness). The product is expected to be a racemic mixture due to the achiral nature of the OSDA. The projection symmetries along [100] and [111] directions are $p4gm$ and $p3m1$, respectively, determined from the phases extracted from Fourier transforms of HRTEM images using CRISP,²⁴ which further confirmed the space group. The projected potential maps show clearly the pore structure that is consistent with the structure model (Supplementary Fig. S1 and S10).

Structure Determination. PXRD data were collected on a PANalytical X'Pert Pro. The structure was solved by charge-flipping algorithm combining SAED intensities and PXRD using the Superflip program.²⁰ The final structure model was refined by Rietveld refinement using TOPAS²⁵ with soft restraints for bond distances considering Si/Ge occupancies. All T positions were refined with mixed occupancies of Si and Ge and a fixed overall Si/Ge ratio of 1.40 according to the elemental analysis. The OSDAs could not be located due to their partial occupancies and lower symmetry. Instead, 15 unique carbon atoms were added at random positions inside the pores and refined subsequently. The PXRD pattern of the calcined sample also agrees with the structure model, but the diffraction peaks were too broad in the high angle region to perform a good refinement. This is due to the collapse of three-connected T atoms.¹⁷

Acknowledgements This project is supported by the CICYT (Project MAT 2006-14274-C02-01), the Swedish Research Council (VR) and the Swedish Governmental Agency for Innovation Systems (VINNOVA). J.-L. Sun and C. Bonneau are supported by post doc grants from the Carl-Trygger Foundation and Wenner-Gren Foundation respectively. M. Moliner thanks ITQ for a scholarship.

Author Contributions D.-L.Z. and M.-R.L carried out the TEM work. J.-L.S. executed the structure solution and refinement. C.B. realised the topological analysis. M.M., M.J. D. and A. C carried out the zeolite synthesis work. A.C. synthesized the OSDA. J. -L.S., C. B., A.C. and X. D. Z were responsible for the redaction of the manuscript.

Author Information Reprints and permissions information is available at npg.nature.com/reprintsandpermissions. The authors declare no competing financial interests. Correspondence and requests for materials should be addressed to A.C (acorma@itq.upv.es) or X.D.Z. (zou@struc.su.se).

References

1. Davis, M. E. Ordered porous materials for emerging applications. *Nature* **417**, 813-821 (2002).
2. Corma, A. State of the art and future challenges of zeolites as catalysis. *J. Catal.* **216**, 298-312 (2003).
3. Férey, G. Materials science: The simplicity of complexity - rational design of giant pores. *Science* **291**, 994-995 (2001).
4. Corma, A., Díaz-Cabañas, M. J., Jorda, J. L., Martínez, C. & Moliner, M. High-throughput synthesis and catalytic properties of a molecular sieve with 18- and 10-member rings. *Nature* **443**, 842-845 (2006).
5. Tang, L. *et al.* A zeolite family with chiral and achiral structures built from the same building layer. *Nature Mater.* **7**, 381-385 (2008).
6. Baerlocher, Ch., McCusker, L.B. & Palatinus, L. Charge flipping combined with histogram matching to solve complex crystal structures from powder diffraction data. *Z. Kristallogr.* **222**, 47-53 (2007).
7. Delgado-Friedrichs, O., O'Keeffe, M. & Yaghi, O. M. Three-periodic nets and tilings: regular and quasiregular nets. *Acta Crystallogr. A* **59**, 22-27 (2003).
8. Schröder, G.E. Fogden, A. & Hyde, S.T. Bicontinuous geometries and molecular self-assembly: Comparison of local curvature and global packing variation in genus-three cubic, tetragonal and rhombohedral surfaces. *Eur Phys. J. B* **54**, 509-524 (2006).
9. Taylor, W.H. The structure of analcite (NaAlSi₂O₆.H₂O) *Z. Kristallogr.* **74**, 1-19 (1930)
10. Gier, T.E., Bu, X., Feng, P., Stucky, G.D. Synthesis and organization of zeolite-like materials with three-dimensional helical pores. *Nature* **395**, 154-157 (1998).
11. Zou, X., Conradsson, T., Klingstedt, M., Dadachov, M.S. & O'Keeffe, M. A mesoporous germanium oxide with crystalline pore walls and its chiral derivative. *Nature* **437**, 716-719 (2005).
12. O'Keeffe, M., Peskov, M. A., Ramsden, S. J., Yaghi, O. M. The Reticular Chemistry Structure Resource (RCSR) Database of, and Symbols for, Crystal Nets, *Acc. Chem Res.*, Article ASAP (2008).

13. Cantin, A., Corma, A., Diaz-Cabanas, M. J., Jorda, J. L. & Moliner, M. Rational design and HT techniques allow the synthesis of new IWR zeolite polymorphs. *J. Am. Chem. Soc.* **128**, 4216-4217 (2006).
14. Gramm, F. *et al.* Complex zeolite structure solved by combining powder diffraction and electron microscopy. *Nature* **444**, 79-81 (2006).
15. Baerlocher, Ch. *et al.* Structure of the polycrystalline zeolite catalyst IM-5 solved by enhanced charge flipping. *Science* **315**, 1113-1116 (2007).
16. Baerlocher, Ch. *et al.* Ordered silicon vacancies in the framework structure of the zeolite catalyst SSZ-74, *Nature Mater.* **7**, 631-635 (2008).
17. Grosse-Kunstleve, R.W., McCusker, L. B. & Baerlocher, Ch. Powder diffraction data and crystal chemical information combined in an automated structure determination procedure for zeolites. *J. Appl. Crystallogr.* **30**, 985-995 (1997).
18. Palatinus, L. & Chapuis, G. Superflip - a computer program for the solution of crystal structures by charge flipping in arbitrary dimensions. *J. Appl. Crystallogr.* **40**, 786-790 (2007).
19. Zou, X.D., Sukharev, Y. & Hovmöller, S. Quantitative measurement of intensities from electron diffraction patterns for structure determination - new features in the program system ELD. *Ultramicroscopy* **52**, 436-444 (1993).
20. Baerlocher, Ch., McCusker, L. B. & Palatinus, L. Charge flipping combined with histogram matching to solve complex crystal structures from powder diffraction data. *Z. Kristallogr.* **222**, 47-53 (2007).
21. Delgado-Friedrichs, O. & O'Keeffe, M. Identification and symmetry computation for crystal nets. *Acta Crystallogr. A* **59**, 351-360 (2003).
22. Delgado-Friedrichs, O. Data structures and algorithms for tilings I. *Theoretical Computer Science* **303**, 431-445 (2003).
23. Blatov, V. A. Multipurpose crystallochemical analysis with the program package TOPOS. *IUCr CompComm Newsletter* **7**, 4-38 (2006).
24. Hovmöller, S. CRISP: Crystallographic image processing on a personal computer. *Ultramicroscopy* **41**, 121-135 (1992).
25. Young, R.A. The Rietveld Method. IUCr Book Serials, Oxford University Press (1993).

Figure 1 The framework and corresponding nets of ITQ-37. **a**, A slice (15.3 Å thick) viewed down the [111] direction. Only the T-T connections and oxygen atoms belonging in the terminal hydroxyl groups are shown. **b**, The largest 30-ring with an opening of 4.7×19.7 Å in which one tertiary building unit $T_{44}O_{145}(OH)_7$ is highlighted. Each tertiary building unit consists of one unique 4^26^4 (lau) cage (in gold) and two unique D4Rs (in green), generated by a 3-fold rotation operation passing through one of the body diagonal of the D4R1. Each D4R1 contains one terminal hydroxyl group and each D4R2 contains two terminal hydroxyl groups as shown in **a**. The 30-ring is built from ten such tertiary building units. The centres of the tertiary building units fall on a **srs** net (in orange). **c**, The resulting channel system, also a **srs** net (in blue), corresponds to the enantiomer of the framework,

Figure 2. Tiling of ITQ-37. **a**, The tertiary building unit $T_{44}O_{145}(OH)_7$ built from one D4R1, three D4R2 and Lau cages 4^26^4 cage (lau). **b**, Tiles of the tertiary building unit in **a**. The interfacial tiles (6^3) are omitted for clarity. -OH bearing T atoms were omitted for the tiling computation. **c**, Tiling of the framework (green and brown) and the channel system (blue) showing the large pore volume compared to the framework wall. The framework and channel systems have opposite chirality (left-handedness for the framework while right-handedness for the channel system). **d**, The **srs** large cavity defined by three 30-ring.

Figure 3 Electron density map derived by charge-flipping algorithm and the obtained structure model, both are viewed along the *c*-axis. **a**, The electron density map is represented by two iso-surfaces at $2.7e/\text{Å}^3$ (in red) and $0.7e/\text{Å}^3$ (in blue), respectively (the maximum and minimum electron densities are $5.5 e/\text{Å}^3$ and $-0.7 e/\text{Å}^3$, respectively). All T (Si and Ge) and 18 out of 19 O atoms could be directly located from the map. **b**, The framework structure model of ITQ-37 deduced from **a**. The T-atoms are in yellow and oxygen atoms are in red.

Figure 4 Observed (blue), calculated (red) and difference (black) PXRD profiles for the Rietveld refinement of the as-synthesized ITQ-37 ($\lambda = 1.5406$ Å). The higher angle data ($2\theta = 30-80^\circ$) has been scaled up (inset) in order to show the good fit between observed and calculated patterns. The low-angle region (not shown, containing only two peaks 011 and 111) were excluded in the refinement due to the uncertainty of these low angle data.

METHODS

1.-Synthesis of the OSDA

Synthesis SDA1, and SDA2

The starting materials for the synthesis of SDA1, and SDA2, were bicyclo[2.2.1]oct-7ene-2,3,5,6-tetracarboxylic dianhydride, and 4,6-Dimethyl- α -pyrone and maleic anhydride, respectively.

Synthesis of Diels-Alder adduct from 4,6-Dimethyl- α -pyrone and maleic anhydride. A toluene solution (500 mL) of 4,6-Dimethyl- α -pyrone (161 mmol) and maleic anhydride (322 mmol) was refluxed for 5 days. After cooling, the resulting precipitate was filtered and washed with hexane to give the corresponding bicyclodianhydride (87%).

Amination of bicyclodianhydrides. Bicyclodianhydride products (140 mmol) were dissolved in ethylamine solution (70% in H₂O) (400 mL) and refluxed for 3.5 days. After cooling, the solvent was eliminated in the rotary evaporator providing the desired diimides in quantitative form.

Reduction of diimides. To a suspension of LiAlH₄ (244 mmol) in anhydrous THF (300 mL) was slowly added the corresponding diimide (49 mmol) under N₂ and at 0° C. When the addition was finished the mixture was refluxed for 5 hours and stirred at room temperature overnight. Then, the reaction was quenched by addition of H₂O (10 mL), 15% aqueous solution of NaOH (10 mL) and distilled H₂O (10 mL). After 30 min stirring at room temperature the solution was filtered, partially concentrated in the rotary evaporator and then extracted with dichloromethane. The combined organic extracts were washed with brine, dried and concentrated to dryness providing the corresponding amines (66%).

Alkylation of the diamine. Iodomethane (642 mmol) was added over a solution of diamine (52 mmol) in 70 ml of methanol. The mixture was stirred at room temperature for 72 hours and after that a new addition of the same amount of methyl iodide was added and kept under stirring 72 hours. Then, the final organic dication was concentrated under vacuum and precipitated by addition of diethyl ether. The precipitate was filtered under vacuum yielding to 20.8 g (89%) of the diquaternary ammonium as di-iodide salt

Synthesis SDA3

The starting materials for the synthesis of SDA3 were N-methylmaleimide and benzene.

Cycloaddition of N-methylmaleimide and benzene. A solution of N-methylmaleimide (108 mmol) in a mixture of benzene (300 mL), acetophenone (30 mL) and acetone (84 mL) was distributed in 10 Pyrex tubes. Prior to the photochemical reaction, N₂ was flowed through the solutions for 15 minutes and, afterwards, were irradiated under stirring with a high pressure Hg lamp ($200 < \lambda < 90$ nm) during 48 hours. The resulting precipitate was filtered under vacuum providing the desired diimide (40 %).

Reduction of the diimide. To a suspension of LiAlH₄ (244 mmol) in anhydrous THF (300 mL) was slowly added the corresponding diimide (49 mmol) under N₂ and at 0° C. When the addition was finished the mixture was refluxed for 5 hours and stirred at room temperature overnight. Then, the reaction was quenched by addition of H₂O (10 mL), 15% aqueous solution of NaOH (10 mL) and distilled H₂O (10 mL). After 30 min stirring at room temperature the solution was filtered, partially concentrated in the rotary evaporator and then extracted with dichloromethane. The combined organic extracts were washed with brine, dried and concentrated to dryness providing the corresponding diamine (70%).

Alkylation of the diamine. To a solution of the diamine (33.5 mmol) in methanol (85 mL) was added CH₃I (1.7 mol). The mixture was stirred 7 days at room temperature. The mixture is concentrated under vacuum obtaining the desired diammonium salt (75%).

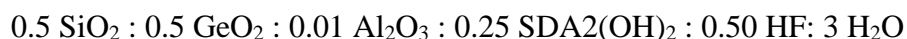
2.- Synthesis of zeolites

Synthesis gels were prepared using the automatic system, composed of a robotic arm for vials handling and solid weighting, a stirring station for gel homogenization and evaporation, a liquid dosing station equipped with pumps and an analytical balance.

Typical automatic synthesis procedure is: boric acid (99.5%, Aldrich) or alumina (74.6%, Condea) is dissolved in the SDA hydroxide solution. Then colloidal silica (Ludox AS-40, Aldrich) is added, and finally, a solution of NH₄F (98%, Aldrich).

The synthesis gel was introduced inside Teflon vials (3 ml), which were finally inserted in a 15 well multiautoclave. Crystallization was carried out at 175°C under static conditions. After filtration, washing and drying, the samples were characterized by PXRD using a multi-sample Phillips X'Pert diffractometer employing Cu K α radiation.

The composition of a typical synthesis gel to obtain ITQ-37 was:



Crystallization was carried out at 175°C during 24 hours under static conditions.

3.- Catalytic experiments

Activation of 100 mg. of the catalyst was performed *in situ* by heating at 110°C the solid under vacuum for 3 h. After this time, the system was left at room temperature and then a solution of the carbonyl compound (Aldrich) (3 mmol) and triethyl orthoformate (98%, Aldrich) (11 mmol) in tetrachloromethane (Panreac) (25 ml) as solvent was poured onto the activated catalyst. The resulting suspension was magnetically stirred at reflux temperature. Aliquots were analyzed at different reaction times by means of gas chromatography (HP-5 column), while products were identified by mass spectroscopy. Response factors of the different compounds were determined to accurately calculate the conversion and selectivity of the process.